

Constrained Convergent Gait Regulation for a Climbing Robot

Salomon Trujillo, Barrett Heyneman and Mark Cutkosky
Center for Design Research, Stanford University
Stanford, CA 94305–2232, USA
Email: sjtrujil@stanford.edu

Abstract—The priorities of a climbing legged robot are to maintain a grasp on its climbing surface and to climb efficiently against the force of gravity. These priorities profoundly constrain the choice of gaits and gait regulation methods. We propose a gait regulation and analysis method that varies foot detachment timing, effectively modifying stride length and frequency in order to maintain gait phasing, subject to kinematic and stability constraints. The method results in linear equations, leading to straightforward tests for local and global convergence when, for example, disturbances such as foot slippage cause departures from the nominal phasing. We illustrate the procedure with an example involving a bounding gait and compare it with empirical results obtained on the RiSE climbing robot.

I. INTRODUCTION

In comparison to walking or running robots, climbing robots face severe requirements on stability and power consumption. They must maintain contact forces at all times to prevent falling and they must ensure that motors do not overheat when they are climbing rapidly or applying large forces. Therefore, we seek a gait regulation method for climbing robots that will produce convergence to a standard free gait [1], [2], where rhythmic phasing between legs is formulated as an objective, subject to constraints.

Stability typically requires that certain combinations of legs remain attached at various times during a stride. In addition, the legs are subject to kinematic constraints (e.g., on maximum and minimum joint angles). When kinematic and stability constraints conflict, it may be necessary for the robot to pause while other legs are brought into contact. In parallel with the stability and kinematic constraints, a climbing robot is subject to constraints on the maximum sustained torques that its motors can produce without overheating. In an earlier study [3], we have previously found that the following approach would minimize motor heating:

- *Stance*: External forces should be distributed evenly between as many legs as possible, to reduce the maximum heat produced in the motors of any leg.
- *Swing*: The legs should recycle as fast as possible. This approach reduces the total heat produced, when averaged over a full stride period.

Taken together, stability and force distribution requirements govern our choice of gaits and gait regulation methods. Stance calls for a force-controlled approach in order to balance the load between legs and apply the forces needed for grip maintenance. Swing calls for a time-optimal bang-bang controller such that minimal time is spent in swing.

Using these control methods during stance and swing rules out several established methods of gait regulation. However, we still have the freedom to vary attachment and detachment timing. In order to provide the longest potential stride for each leg, we maintain leg attachment at the earliest point possible in the leg’s trajectory. This choice leaves us with the ability to vary leg detachment, effectively altering the stride length and period. In this way, lagging legs will experience faster stride frequencies, and slower frequencies for leading legs, until gait phasing is fully distributed.

Under nominal conditions, we want a gait with evenly spaced footfalls and no pausing. Under difficult conditions, disturbances will alter the phasing between legs and may cause the robot to stop forward movement in order to safely cycle its legs. By implementing a standard gait, the robot maximizes the phase differences between legs for which kinematic and stability constraints may conflict, granting the robot leeway for disturbance rejection. In this article, we will analytically show that our algorithm, for certain parameters, has global convergence and has no undesirable local minima. This analysis can both indicate if a set of gait parameters is globally convergent and give estimates to the rate of convergence. We have implemented our algorithm on a quadruped variant of the RiSE robot V2 [4] and use it to illustrate our approach.

A. Previous Work

The literature for gait regulation in the context of legged robots is extensive [5], [6], [7], [8]. It is undesirable to simply encode position trajectories into the robot, as that method would produce internal forces and reduce the ability of the robot to handle perturbations [9]. One solution is to introduce adjustable clocks [10]. This technique works well but requires the gait regulator to have control authority during recirculation. Another strategy is to use central pattern generators where the gait behavior emerges from a set of coupled oscillators [11]. These systems can be difficult to construct when a particular behavior is desired, but they have inspired a series of methods that seek to modify the behavior of legs based on behavior of neighboring legs [12], [13]. The approach modifies various parameters of the gait, including the “posterior extreme position,” which is equivalent to modifying detachment timing in the approach that we present here. Unlike these previous approaches, we employ a centralized controller, including a novel gait representation, that monitors the phases of all legs and triggers detachments.

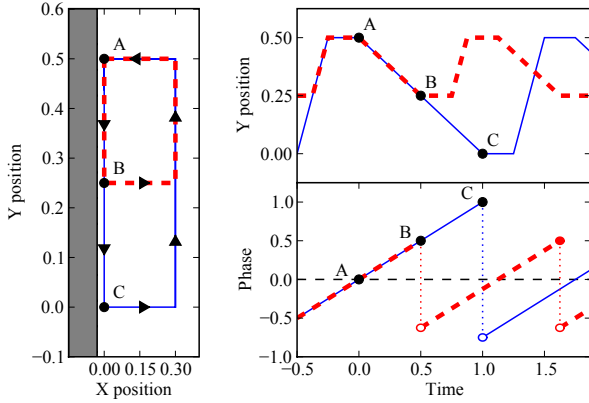


Fig. 1. Left: Simplified leg trajectory for one leg of a climbing robot (grayed surface indicates the wall). Upper-right: Stroke position vs. time. Lower-right: Leg phase, ϕ , vs. time. Note the constant slope of $\phi(t)$ and discontinuities at detachment events.

II. ALGORITHM IMPLEMENTATION

A. Phase

We begin our discussion by presenting our definition of phase. Due to the cyclic nature of legged locomotion, phase is usually treated with the same notation as rotation [14]. Since our method has a continually changing period, it becomes difficult to describe the state in terms of angles or ratios. Instead, we describe phase, ϕ , in units of time as a measure of position, θ , using an approach similar to the phase coordinates of intermittent systems [15]. Using desired leg trajectories, f , parameterized in terms of time, we calculate phase from the inverse of these trajectory functions:

$$\theta_{desired} = f(t) : \phi(t) = f^{-1}(\theta_{actual}) + c \quad (1)$$

To simplify the mathematics, we leave phase in units of time and do not divide by the stride period. During normal operation, the time-derivative of phase is constant, $\frac{d\phi}{dt} \approx 1$, but when a disturbance is encountered, the position of the leg and not the elapsed time determines the perturbation to phase. Since the legs are operating using methods such as force control or bang-bang control and not position control, such perturbations arise frequently.

Fig. 1 shows a schematic representation of a leg trajectory (abstracted here to a rectangular loop for ease of depiction) and the corresponding plots of Y position (stroke along wall) and phase as functions of time. We fix the origin, $\phi = 0$, at the attachment point. This choice provides a convenient notation where positive phase represents a leg in stance while negative phase represents a leg in swing. In theory, the phase function experiences no discontinuity during the attachment event. The detachment point, as shown in Fig. 1, occurs at variable points in state-space and produces a large discontinuity as the phase jumps from the positive stance phase to the negative swing phase.

We model the change in phase at detachment as a linear equation in terms of phase. We assume the durations of attachment, detachment and acceleration and deceleration

are constant and their combined time is represented as δ . Nominal stance and swing velocities (v_{st} and v_{sw}) are fixed as a property of the gait. If a leg that attached at time 0 detaches at time t_d , it has traveled a distance of $v_{st}t_d$ and thus the time it will take to return to the attachment point is $t_d \left| \frac{v_{st}}{v_{sw}} \right| + \delta$. For ease of notation we define the ratio between support and recycling velocities as $\beta = \frac{v_{st}}{v_{sw}}$. We can therefore express detachment as a discontinuous jump in phase:

$$\phi(t_{d+}) = -\beta\phi(t_{d-}) - \delta \quad (2)$$

Building upon the description of phase for a single leg, we represent leg configurations for the robot using a vector of phases in which the phase of the i^{th} leg is ϕ_i .

B. Gait Regulation (GR) Rule

The Gait Regulation rule (hereafter, the GR rule) governs leg detachment. When the weighted average of all the leg phases exceeds a prescribed trigger point, the leg with highest phase should detach. For gaits such as the alternating tripod of a hexapod, a detachment event triggers simultaneous detachment of a set of legs. In order to maintain symmetry with each step, the weighted average is applied to a sorted list of leg phases. We find a permutation of phases that reorders them in descending order: $\psi_i = \phi_j \text{ st. } \psi_1 \geq \psi_2 \geq \dots \geq \psi_n$. The GR rule is written as follows:

$$\sum \omega_i \psi_i \geq T \quad (3)$$

An appropriately chosen GR rule produces rhythmic behavior upon convergence of the gait and distributes the footfalls to maintain sufficient space for accommodating disturbances. However, while it regulates the interactions among legs, it does not prevent the robot from falling. Thus, the GR rule can be preempted by constraints that ensure the stability of the robot.

C. Configuration Constraint (CC) Rules

Under various conditions, the GR rule may fail to trigger a detachment before a leg reaches a joint limit, or it may trigger one that would cause the robot to lose stability. To prevent such situations, we introduce Configuration Constraint (CC) rules that take priority over the GR rule. There are two variants: rules that trigger a detachment and rules that inhibit detachment events.

Obedience to the joint limits is an example of the former variant. Triggering detachment earlier than indicated by the GR rule allows the robot to continue climbing even if a leg runs out of travel. Such a CC rule can be written as

$$\phi_i \geq L_i \quad (4)$$

where i is the index of an arbitrary leg and L_i is that leg's joint limit in phase space. Hereafter, we will assume all joint limits L_i are equal to L . The joint limits define the boundaries of the n -dimensional workspace of the robot, W :

$$L \geq \phi_i \geq -\beta L - \delta \quad (5)$$

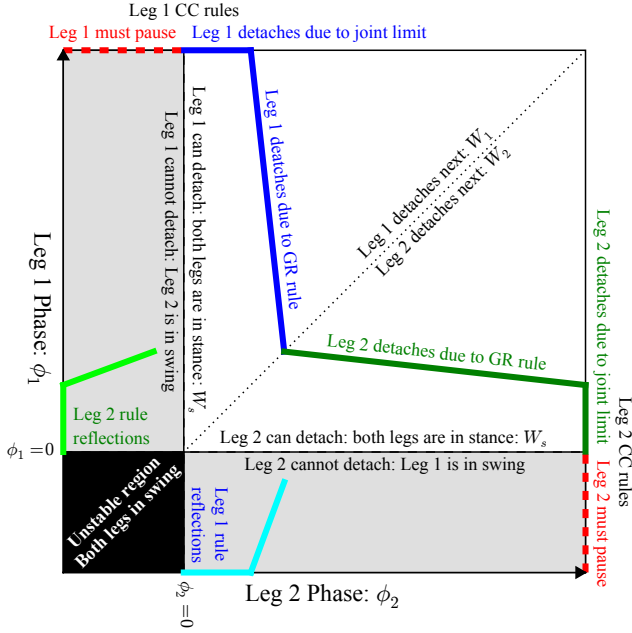


Fig. 2. Annotated phase space for a two-legged robot. The dark solid lines trigger detachment, which instantly shifts the phase to the respective light solid lines.

The second type of CC rule inhibits detachment events that would remove legs essential for support. While the conditions for stability typically depend on the details of the robot and the climbing surface, the gait regulation algorithm only requires that they can be represented by a set of linear inequalities in terms of phase:

$$\sum c_i \phi_i > c_0 \quad (6)$$

The region of the robot workspace, W , in which no inhibitory CC rule is active is referred to as W_s and includes all configurations in which detachment is allowed.

The inhibitory CC rules clearly override the GR rule, as stability is essential. However, more complex cases can also arise, as when a leg hits a joint limit, but its support is needed for stability. If two CC rules produce a conflict, the robot cannot continue to produce forward motion; all legs in stance should halt and wait for the legs in swing to reattach such that the offending leg(s) are not required for support.

III. TWO-LEGGED EXAMPLE

We illustrate the approach for gait regulation in the context of a climbing robot with two virtual legs [19], for which the phase space is conveniently represented with two-dimensional diagrams. For the quadrupedal RiSE robot variant used in the subsequent empirical examples, this simplification corresponds to a bound gait in which the front and rear legs move together. The algebraic method extends straightforwardly to larger numbers of legs, but the phase diagrams become difficult to visualize.

Because the RiSE robot has a tail, either the front or rear pair of legs can hold it against the wall, pulling inward and upward against gravity. Therefore the stability requirement

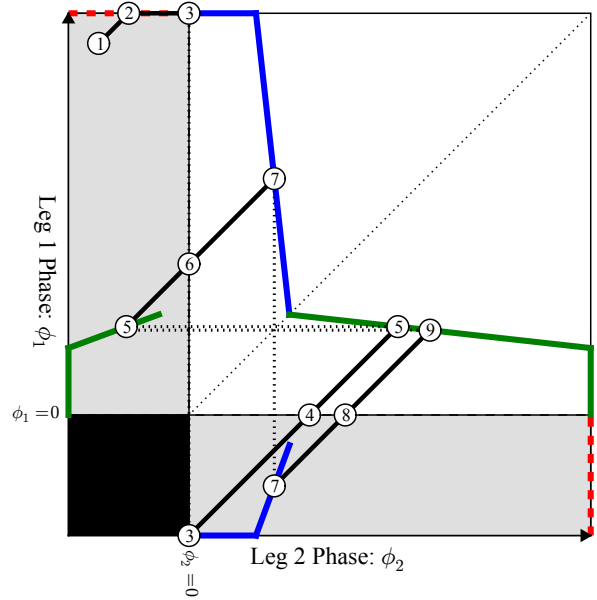


Fig. 3. A sample sequence of events in a converging gait: (1.) The initial configuration of the robot. (2.) Leg 1 strikes a joint limit, but cannot detach because leg 2 is in swing. (3.) Leg 2 attaches, triggering detachment in Leg 1. (4.) Leg 1 attaches. (5.) GR rule triggers detachment in Leg 2. (6.) Leg 2 attaches. (7.) GR rule triggers detachment in Leg 1. (8.) Leg 1 attaches. (9.) GR rule triggers detachment in Leg 2. Events 5 and 9 are very close together indicating that they are near the equilibrium path of the gait.

is that at least one virtual leg be in stance. In phase space, the stable region formed is equivalent to the Stance Complex presented in [16]:

$$W_s \equiv \{\vec{\phi} \in W \mid \phi_1 \geq 0, \phi_2 \geq 0\} \quad (7)$$

The work space, W , for the two-legged robot is shown as the white square region in Fig. 2, along with the bounding GR and CC rules. These rules manifest as line segments in W (in higher dimensions, they would appear as $n - 1$ polygonal facets.) The rules are given as linear inequalities, thus they can be used to describe polygonal regions where the rule will trigger detachment [?]. The interior regions are unreachable except by an initial configuration, thus we will only concentrate on their leading edges.

The workspace is split into two regions: $W_1 \equiv \{\vec{\phi} \in W \mid \phi_1 > \phi_2\}$ and $W_2 \equiv \{\vec{\phi} \in W \mid \phi_2 > \phi_1\}$ which are the only orderings of two legs. Since the GR rule operates on the ordered phases, it manifests as symmetric around the boundary between W_1 and W_2 . The slope of the GR rule is defined by the weights ω_i . The CC rule appears on the joint-limit boundary of W .

In this example, we mark segments of the rules that trigger detachment with a solid line. The dashed lines represent boundaries where the joint limit CC rule and the stability CC rule conflict, forcing the robot to pause instead of detaching a leg. For rules that do trigger detachment, we can geometrically show the result by applying the detachment transformation (2) to the line segments.

Fig. 3 shows several steps of the robot whose gait converges quickly. The phase vector of the robot almost always travels in the same direction since $\frac{d\phi_i}{dt} = 1$, except when CC rules conflict or a detachment creates a discontinuous jump.

IV. CONVERGENCE ANALYSIS

We present two analysis techniques. The algebraic method, which extends easily to multiple legs, will determine whether the gait will converge locally to an equilibrium path. The geometric method can be used to test for global convergence from any starting configuration. It also extends to larger numbers of legs, although the diagrams become increasingly complex.

A. Algebraic Method

For algebraic analysis we use the sorted phases, ψ_i and express them in homogeneous coordinates [17]:

$$\vec{\psi}(t) = [\psi_1(t) \quad \psi_2(t) \quad \dots \quad \psi_n(t) \quad 1]^T \quad (8)$$

We construct matrix operators for $\vec{\psi}$ that compute subsequent states given an initial state. The sorted vector allows us to examine the effect of a single footstep, but requires operators that maintain the sorting.

In a gait that detaches m legs at a time, the one with the highest phase, ψ_1 , detaches first, along with an additional $m - 1$ legs that are determined by the gait. We assume that upon convergence these m legs are in phase with each other and thus have the highest phases $\psi_i \dots \psi_m$. The phase is modified by application of (2), and $\vec{\psi}$ is reordered to maintain its sorting. These two operations are performed simultaneously by the m -leg Detachment Matrix

$$D_m = \begin{bmatrix} 0 & I_{n-m} & 0 \\ -\beta I_m & 0_{m \times n-m} & -\delta \vec{1}_m \\ 0 & 0_{1 \times n-m} & 1 \end{bmatrix} \quad (9)$$

We represent the locomotion of the legs as a constant translation in homogeneous phase coordinates along the vector $[1 \ 1 \ \dots \ 1 \ 0]$. This translation continues until the next GR rule transition, given by (3). The difference between T and the current weighted sum of the leg phases tells us how far each leg will advance, yielding

$$\psi_i^{(k+1)} = \psi_i^{(k)} + \left(T - \sum \omega_i \psi_i^{(k)} \right). \quad (10)$$

This operation can be performed on all the legs by the Translation Matrix

$$L = \begin{bmatrix} I_n - \vec{1}_n \vec{w}^T & T \vec{1}_n \\ \vec{0}_n^T & 1 \end{bmatrix} \quad (11)$$

An example of the construction of these matrices is shown later in (15). Given these two matrices, we construct the Recurrence Matrix, $R_m = LD_m$, which maps an augmented leg-phase vector from one detachment to the next. This matrix is analogous to the Poincaré map, although the underlying system is not continuous.

Once we have R_m we can analyze its eigenvalues to determine convergence of the GR rule. Because we are

using homogeneous coordinates, the construction of R_m guarantees there will always be at least one eigenvalue $\lambda = 1$, and the corresponding eigenvector, $\vec{\xi}(\lambda = 1)$, will be the only eigenvector with a nonzero final entry. When $\vec{\xi}$ is scaled so that its final element is 1, it gives the equilibrium detachment state of the leg phases.

This analysis provides two necessary conditions for the gait to converge to $\vec{\xi}$. First, all other modes must decay [18]: $|\lambda_i| < 1$. Second, $\vec{\xi}$ must be achievable: $\vec{\xi} \in W_s$. If $\vec{\xi} \notin W_s$, then the GR Rule will cause the phase to decay such that it will try to leave W_s . A CC Rule will then cause a transition, thereby preventing the phase from converging to the equilibrium, ξ .

B. Geometric Method

If the gait satisfies the necessary conditions generated by the algebraic analysis, a more involved geometric and graph theory analysis will allow us to establish global convergence. W is segmented into distinct regions, so that each region transitions due to a single rule, progressing to a single new region. The regions can be viewed as nodes in a directed graph, where every node has an out-degree of 1.

The first step in the geometric analysis is to create the boundary of W . Because GR rules operate on the ordered phase vector, $\vec{\psi}$, but points in W are unordered phases, W is divided into $n!$ regions corresponding to each possible leg ordering. Next any inhibitory CC rules are outlined, as well as any unstable regions, to yield W_s .

At this point we begin construction of the transition boundary B , composed of facets associated with GR or CC rules that trigger detachment. First, facets for the GR rules are added in each of the $n!$ regions. Any GR rule facets that lie outside W_s are removed, since an inhibitory CC rule would prevent detachment. Then facets for any detachment CC rules are added to complete B . A complete transition boundary transects W_s ; i.e. the projections of B and W_s onto the plane perpendicular to $[1 \ 1 \ \dots \ 1]$ are equal.

Given B , W can be segmented to satisfy the conditions outlined above. The full details of this segmentation process are not presented here due to space limitations. During segmentation, the directed graph, G , is constructed and each node is categorized according to which rules govern transition from it: *GR nodes* transition due to the GR rule only; *CC nodes* transition due to CC rules.

For the gait to be globally convergent, the robot must be able to start in any configuration and eventually enter a cycle in which it always transitions due to a GR rule. Equivalently, requirements for G are for all cycles in G to include only GR nodes, and for every other node in G to be able to reach one of these cycles. These properties can be checked by inspection or through methods outlined in [?], [18].

If these requirements are satisfied, the robot will reach a GR region within a finite number of steps from any starting region. After reaching the GR region, the detachment state will asymptotically converge to the equilibrium path, as shown by the algebraic analysis. If the requirements are not satisfied, the robot can enter a cyclic gait in which at least

TABLE I
GAIT PARAMETERS USED FOR THE TWO-LEGGED EXAMPLE.

	β	δ	ω_1	ω_2	T	L
Example	0.3	0.15 sec	0.3	0.7	0.16 sec	0.5 sec

one transition is due to a CC rule, and the detachment state will not converge to $\vec{\xi}(\lambda = 1)$.

C. Two-Legged Example Analysis

The parameters for a GR rule are listed in Table I along with the joint limit L . We empirically determine β and δ by first selecting a desired forward velocity and measuring the various velocities and time durations exhibited by the robot. The weights ω and trigger point T are also determined empirically. The synthesis of gaits is beyond the scope of this article, but experience indicates that the the heaviest weights for an n legged robot that lifts m legs at a time should be ω_n and ω_{m+1} (which for the two legged case are the same leg) with a light weight for ω_1 . This approach seems to couple the phase of the leg to the next and previous neighbors in phase.

Using the parameters in Table I, we form the R matrix:

$$R = LD_1 = \begin{bmatrix} 0.21 & 0.7 & 0.265 \\ -0.09 & -0.3 & 0.115 \\ 0 & 0 & 1 \end{bmatrix} \quad (12)$$

The eigenvalues and associated eigenvectors are:

$$\begin{aligned} \vec{\xi}(\lambda = 1) &= [0.390 \ 0.061 \ 1]^T \\ \vec{\xi}(\lambda = -0.09) &= [7 \ -3 \ 0]^T \\ \vec{\xi}(\lambda = 0) &= [10 \ -3 \ 0]^T \end{aligned} \quad (13)$$

This system is locally convergent because we have a single eigenvalue equal to 1 while the rest have absolute values less than one and $\vec{\xi}(\lambda = 1) \in W_s$. This eigenvector describes the equilibrium phases of the legs before detachment, while the others describe transient modes that decay.

The algebraic analysis has demonstrated convergence in the neighborhood of equilibrium; we now check for global convergence. Fig. 4 shows the gait space divided into six regions. The boundaries between regions are lines parallel to the phase direction $[1 \ 1]^T$. The boundaries coincide with the boundaries between the various GR and CC rules such that each region meets the requirement of detaching due to a single rule. In addition, each region only maps to a single distinct region, thus we do not need to further segment the gait space. Regions 2 and 3 both transition to region 4 and likewise for 4 and 5 to 3. Regions 1 and 6 encounter the conflicting CC rule boundary, but in these cases, the phase slides along the boundary until it reaches the corners of regions 2 and 5, respectively, which instantaneously triggers detachment. Using these regions, we obtain the directed graph:

$$G : \textcircled{1} \rightarrow \textcircled{2} \rightarrow \boxed{4} \leftrightarrow \boxed{3} \leftarrow \textcircled{5} \leftarrow \textcircled{6} \quad (14)$$

GR nodes are represented by boxes and CC nodes represented by circles. By inspection, the only cycle involves

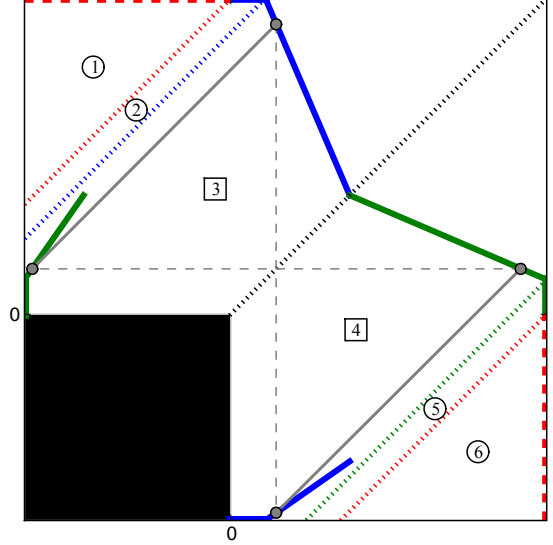


Fig. 4. The 2D gait space using parameters from Table I. Dotted lines indicate the divisions between the regions. Four small gray-filled circles and their connecting lines indicate the equilibrium path.

TABLE II
GAIT PARAMETERS USED FOR THE THE STABLE AND UNSTABLE GAIT.

	β	δ	ω_1	ω_2	ω_3	ω_4	T
Convergent	0.3	0.15 s	0.3	0.3	0.2	0.2	0.27 s
Non-Convergent	0.3	0.15 s	0.5	0.5	0.0	0.0	0.38 s

GR regions 3 and 4, and all other nodes lead to that cycle. Therefore, the gait is globally convergent.

V. RESULTS

We implemented two gaits, one convergent and one non-convergent, on the quadrupedal RiSE robot and compared the observed behavior with predictions from the analysis. For these tests, the robot performed a bound but we considered the four legs separately to see the effects of disturbances when a single left or right leg slips. The algebraic analysis extends easily to the four-legged description using a 5×5 matrix but the geometric analysis requires a 4D representation of the phase space and is not shown here. The GR rule, with parameters from Table II, governs the bounding gait and synchronizes the left and right legs.

Applying (9), we get the detachment matrix, LD :

$$\begin{bmatrix} 1 - \omega_1 & -\omega_2 & -\omega_3 & -\omega_4 & T \\ -\omega_1 & 1 - \omega_2 & -\omega_3 & -\omega_4 & T \\ -\omega_1 & -\omega_2 & 1 - \omega_3 & -\omega_4 & T \\ -\omega_1 & -\omega_2 & -\omega_3 & 1 - \omega_4 & T \\ 0 & 0 & 0 & 0 & 1 \end{bmatrix} \begin{bmatrix} 0 & 0 & 1 & 0 & 0 \\ 0 & 0 & 0 & 1 & 0 \\ -\beta & 0 & 0 & 0 & -\delta \\ 0 & -\beta & 0 & 0 & -\delta \\ 0 & 0 & 0 & 0 & 1 \end{bmatrix} \quad (15)$$

A. Convergent Gait

We substitute the “convergent” values from Table II and form $R = LD$ to yield the eigenvalues:

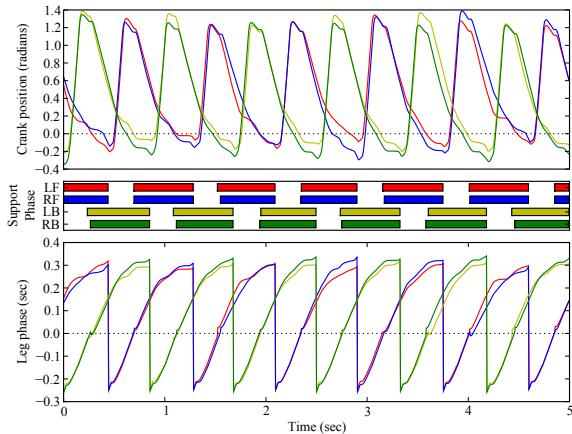


Fig. 5. The robot begins climbing using a convergent GR rule.

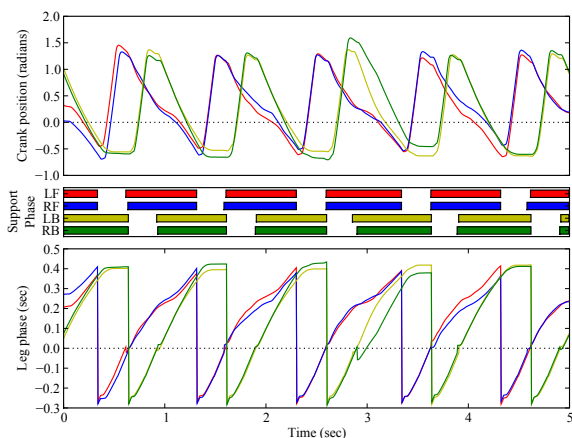


Fig. 6. The robot begins climbing using a non-convergent GR rule. Note that back pair must pause and wait for the front pair to attach.

$\begin{bmatrix} 0.55i & -0.55i & 0 & -0.48 & 1 \\ 0.41 & 0.41 & 0.06 & 0.06 & 1 \end{bmatrix}^T$. According to our criteria in Section IV-A, this gait is locally convergent. As the equilibrium detachment phase vector shows, the gait keeps the front and rear out of phase with each other and keeps the left and right leg pairs in phase.

Fig. 5 shows the gait at steady-state. There are a few disturbances in the phase function during attachment because the legs do not always reattach at the same spot. Also, as the robot climbs it experiences different loading conditions for each step, so every footfall looks different. There may also be predictable but unmodeled discrepancies between the internal model and the physical leg trajectories. Despite these errors, the gait converges readily.

B. Non-Convergent Gait

The eigenvalues for R using the non-convergent parameters are $\begin{bmatrix} -1 & 0.55i & -0.55i & 0 & 1 \end{bmatrix}$. The eigenvector associated with the -1 eigenvalue is $\begin{bmatrix} 0 & 0 & 1 & 1 & 0 \end{bmatrix}$.

Since there are two eigenvalues with absolute values of one, the system will not converge to a single equilibrium path. Fig. 6 shows the results of this gait, which, as predicted, does not produce a symmetric gait. However, since the algorithm protects the robot from entering a fatal configuration, the robot can still climb.

These parameters correspond to a gait in which the front and back legs are uncoupled. Further, because RiSE is non-ideal, different legs move with slightly different speeds during swing. Because the GR rule does not couple the front and back legs, the faster pair is able to catch up to the slower pair and a stability CC rule forces them to stay in stance until the slower pair has attached.

It should be noted that due to the CC rules, the robot should never fall due to lack of proper foot placement. However, because the gait is effectively regulated by the CC rules, which have no stability margin, it is at increased risk. In addition, this gait increases the likelihood of losing forward momentum due to a slip or a disturbance. As shown in Fig. 6, the front pair of legs is trailing the rear pair and cannot not recycle until the rear pair attaches. If the front legs slip and advance in phase, they may hit a joint limit and need to pause while waiting for the rear legs to attach. The result can be seen as undesirable flat spots in the plot of crank position versus time. In contrast, with leg detachments spaced as in Fig. 5, the front pair has to slip much further for this condition to arise.

VI. CONCLUSIONS AND FUTURE WORK

We presented an algorithm for gait regulation for a climbing legged robot that operates under practical considerations imposed by stability and motor thermal optimization. Subject to these considerations, the algorithm regulates the gait by varying leg detachment timings. We present algebraic and geometric tests for local and global convergence to a standard free gait [1], which yields an even rhythm and is robust against disturbances. The algorithm is designed to ensure the robot remains stable at all times, even when a gait is unable to converge. We presented the method in the context of a robot with two virtual legs and tested it on a four-legged variant of the RiSE robot.

We plan to extend this algorithm to different gaits with larger numbers of legs. The approach should be also suitable to for different types of legged robots, including walking robots that are not as thermally constrained. We plan to extend the geometric analysis tools for larger numbers of dimensions, for which the representation of the phase space is no longer as easy to inspect. We are also interested in dynamically switching between different gaits and sets of parameters. Finally, while the approach presented here provides for gait analysis, the synthesis of new gaits is an important and more open-ended problem for future work.

VII. ACKNOWLEDGMENTS

The authors thank the members of the Biomimetics and Dexterous Manipulation Laboratory for their advice during this project and Robin D. Trujillo for support and editing.

The RiSE project was supported by the DARPA BioDynamics Program. Trujillo is partially supported by the Alfred P. Sloan Foundation.

REFERENCES

- [1] S. Hirose, Y. Fukuda, and H. Kikuchi, "The gait control system of a quadruped walking vehicle," *Advanced robotics*, Jan 1986.
- [2] S. Hirose and O. Kunieda, "Generalized Standard Foot Trajectory for a Quadruped Walking Vehicle," *The International Journal of Robotics Research*, vol. 10, no. 1, pp. 3–12, 1991. [Online]. Available: <http://ijr.sagepub.com/cgi/content/abstract/10/1/3>
- [3] S. Trujillo and M. Cutkosky, "Thermally constrained motor operation for a climbing robot," *Robotics and Automation, 2009. ICRA '09. IEEE International Conference on*, pp. 2362 – 2367, Apr 2009.
- [4] M. Spenko, G. Haynes, and J. Saunders, "Biologically inspired climbing with a hexapedal robot," *Journal of Field Robotics*, Jan 2008.
- [5] S. Kajita and B. Espiau, "Legged robots," *Springer Handbook of Robotics*, pp. 361–389, 2008. [Online]. Available: http://dx.doi.org/10.1007/978-3-540-30301-5_17
- [6] A. Calvitti and R. Beer, "Analysis of a distributed model of leg coordination," *Biological Cybernetics*, Jan 2000.
- [7] H. Chiel, R. Beer, R. Quinn, and K. Espenschied, "Robustness of a distributed neural network controller for locomotion in a hexapod robot," *IEEE Transactions on robotics and automation*, Jan 1992.
- [8] T. Roggendorf, "Comparing different controllers for the coordination of a six-legged walker," *Biological cybernetics*, Jan 2005.
- [9] K. Waldron, "Force and motion management in legged locomotion," *Robotics and Automation, IEEE Journal of*, vol. 2, no. 4, pp. 214 – 220, Dec 1986.
- [10] G. Haynes and A. Rizzi, "Gait regulation and feedback on a robotic climbing hexapod," *Proceedings of Robotics: Science and Systems*, Jan 2006.
- [11] M. Frasca, P. Arena, and L. Fortuna, "Bio-inspired emergent control of locomotion systems," Jan 2004.
- [12] H. Cruse, T. Kindermann, M. Schumm, and J. Dean, "Walknet—a biologically inspired network to control six-legged walking," *Neural Networks*, Jan 1998.
- [13] K. Wait and M. Goldfarb, "A biologically inspired approach to the coordination of hexapedal gait," *2007 IEEE International Conference on Robotics and ...*, Jan 2007.
- [14] S. Song and K. Waldron, "An analytical approach for gait study and its applications on wave gaits," *The International Journal of Robotics Research*, Jan 1987.
- [15] E. Klavins and D. Koditschek, "Phase regulation of decentralized cyclic robotic systems," *The International Journal of Robotics Research*, Jan 2002.
- [16] G. C. Haynes, F. R. Cohen, and D. E. Koditschek, "Gait transitions for quasi-static hexapedal locomotion on level ground," *International Symposium of Robotics Research*, 2009.
- [17] D. H. Ballard and C. M. Brown, "Computer vision," pp. 467–481, Jan 1982.
- [18] G. Strang, "Linear algebra and its applications," p. 487, Jan 2006.
- [19] M. Raibert, M. Chepponis, and H. Brown, "Running on four legs as though they were one," *Robotics and Automation, IEEE Journal of*, vol. 2, no. 2, pp. 70 – 82, Jan 1986.